Resssonâncias

Mecânica Clássica

L. Reichl

The Transition to Chaos
Capítulo 2

2.3.3 *Poincaré Surface of Section*

How can we tell if a system is integrable or not? There is no simple way in general. For systems with two degrees of freedom, we can check numerically by constructing a Poincaré surface of section. To see how this works, let us consider a conservative system (a system with a Hamiltonian independent of time). For such systems, the energy is conserved. The Hamiltonian is then an isolating integral of the motion and can be written

$$H(p_1, p_2, q_1, q_2) = E, \tag{2.3.32}$$

where the energy, E, is constant and restricts trajectories to lie on a three-dimensional surface in the four-dimensional phase space.

¿From Eq. (2.3.32) we can write $p_2 = p_2(p_1, q_1, q_2, E)$. If the system has a second isolating integral,

$$I_2(p_1, p_2, q_1, q_2) = C_2, \tag{2.3.33}$$

¿From Eq. (2.3.32) we can write $p_2 = p_2(p_1, q_1, q_2, E)$. If the system has a second isolating integral,

$$I_2(p_1, p_2, q_1, q_2) = C_2, \tag{2.3.33}$$

where C_2 is a constant, then it too defines a three-dimensional surface in the four-dimensional phase space. Once the initial conditions are given, E and C_2 are fixed and the trajectory is constrained to the intersection of the surfaces defined by Eqs. (2.3.32) and (2.3.33); that is, to a two-dimensional surface in the four-dimensional phase space. If we combine Eqs. (2.3.32) and (2.3.33), we can write $p_1 = p_1(q_1, q_2, E, C_2)$. If we now consider the surface $q_2 = 0$, the trajectory lies on a one-dimensional curve.

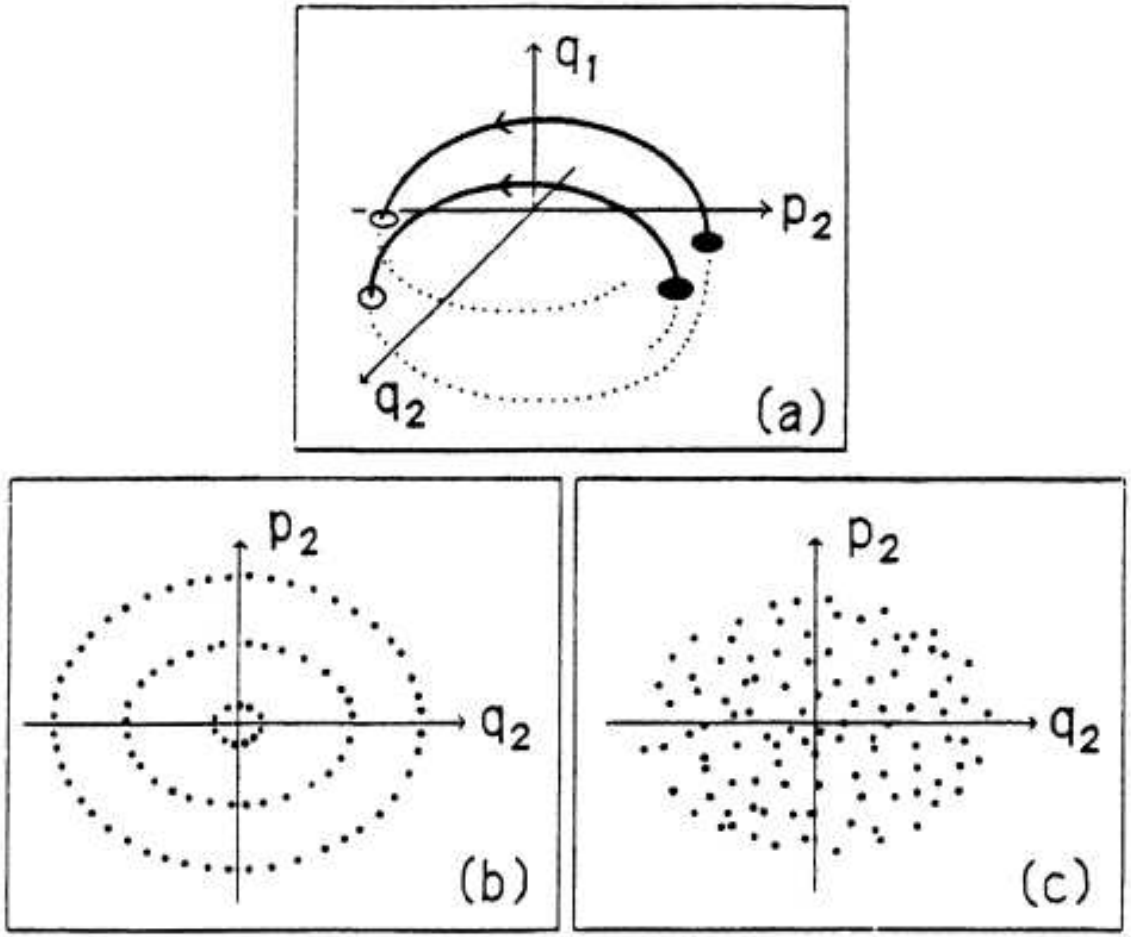

Figure 2.3.1. A Poincaré surface of section for a two degree of freedom system provides a two-dimensional map. (a) A surface of section may be obtained, for example, by plotting a point each time the trajectory passes through the plane $q_1 = 0$ with $p_1 \geq 0$. (b) If two isolating integrals exist, the trajectory will lie along one-dimensional curves in the two-dimensional surface. (c) If only one isolating integral exists (the energy), the trajectory will spread over a two-dimensional region whose extent is limited by energy conservation.

2.4.1 Single-Resonance Hamiltonians

In terms of action-angle variables, a general single-resonance Hamiltonian can be written

$$H = H_0(J_1, J_2) + \epsilon V_{n_1,n_2}(J_1, J_2)\cos(n_1\theta_1 - n_2\theta_2) = E, \tag{2.4.1}$$

where $(J_1, J_2, \theta_1, \theta_2)$ are action-angle variables. This system has a second isolating integral

$$I = n_2 J_1 + n_1 J_2 = C_2, \tag{2.4.2}$$

where C_2 is a constant. It is easy to see that Eq. (2.4.2) is an isolating integral. Write Hamilton's equations of motion for J_1 and J_2,

$$\frac{dJ_1}{dt} = -\frac{\partial H}{\partial \theta_1} = n_1 \epsilon V_{n_1,n_2} \sin(n_1\theta_1 - n_2\theta_2) \tag{2.4.3}$$

and

$$\frac{dJ_2}{dt} = -\frac{\partial H}{\partial \theta_2} = -n_2 \epsilon V_{n_1,n_2} \sin(n_1\theta_1 - n_2\theta_2). \tag{2.4.4}$$

Using Eqs. (2.4.3) and (2.4.4), we find that

$$\frac{dI}{dt} = 0. \tag{2.4.5}$$

(2,2) Resonance

To see more clearly how a resonance works, let us consider the specific case of a (2,2) resonance. Following Walker and Ford, we write the Hamiltonian

$$H = H_0(J_1, J_2) + \alpha J_1 J_2 \cos(2\theta_1 - 2\theta_2) = E, \tag{2.4.6}$$

where

$$H_0(J_1, J_2) = J_1 + J_2 - J_1^2 - 3J_1 J_2 + J_2^2. \tag{2.4.7}$$

It is useful to make a transformation from action-angle variables $(J_1, J_2, \theta_1, \theta_2)$ to a new set of variables $(\mathcal{J}_1, \mathcal{J}_2, \Theta_1, \Theta_2)$ via the canonical transformation $\mathcal{J}_1 = J_1 + J_2 = I' = \frac{I}{2}$, $\mathcal{J}_2 = J_2$, $\Theta_1 = \theta_2$, and $\Theta_2 = \theta_2 - \theta_1$. The Hamiltonian then takes the form

$$\mathcal{H} = \mathcal{J}_1 - \mathcal{J}_1^2 - \mathcal{J}_1\mathcal{J}_2 + 3\mathcal{J}_2^2 + \alpha\mathcal{J}_2(\mathcal{J}_1 - \mathcal{J}_2)\cos(2\Theta_2) = E. \qquad (2.4.8)$$

Since $\mathcal{H}$ is independent of Θ_1, in this new coordinate system $\mathcal{J}_1$ is constant. Hamilton's equations in this coordinate system become

$$\frac{d\mathcal{J}_1}{dt} = 0, \qquad (2.4.9.a)$$

$$\frac{d\Theta_1}{dt} = 1 - 2\mathcal{J}_1 - \mathcal{J}_2 + \alpha\mathcal{J}_2\cos(2\Theta_2), \qquad (2.4.9.b)$$

and

$$\frac{d\mathcal{J}_2}{dt} = 2\alpha\mathcal{J}_2\sin(2\Theta_2)(I' - \mathcal{J}_2), \qquad (2.4.10.a)$$

$$\frac{d\Theta_2}{dt} = -I' + 6\mathcal{J}_2 + \alpha\cos(2\Theta_2)(I' - 2\mathcal{J}_2). \qquad (2.4.10.b)$$

Since $\mathcal{J}_1$ is constant, Eqs. (2.4.10) can be solved first for $\mathcal{J}_2(t)$ and $\Theta_2(t)$ and then substituted into Eq. (2.4.9.b) to obtain $\Theta_1(t)$.

Let us now find the fixed points of these equations. The fixed points are points for which $\frac{d\mathcal{J}_2}{dt} = 0$ and $\frac{d\Theta_2}{dt} = 0$. Fixed points occur when $\Theta_2 = \frac{n\pi}{2}$ and $\mathcal{J}_2 = \mathcal{J}_o$, where $\mathcal{J}_o$ is a solution of the equation

$$-I' + 6\mathcal{J}_o + \alpha\cos(n\pi)(I' - 2\mathcal{J}_o) = 0. \tag{2.4.11}$$

Note that for $\alpha \ll 1$, $\mathcal{J}_o \approx \frac{I'}{6}$.

The nature of the fixed points can be determined by linearizing the equations of motion about points $(\mathcal{J}_2 = \mathcal{J}_o, \Theta_2 = \frac{n\pi}{2})$. We let $\mathcal{J}_2(t) = \mathcal{J}_o + \Delta\mathcal{J}(t)$ and $\Theta_2(t) = \frac{n\pi}{2} + \Delta\Theta(t)$ and linearize in $\Delta\mathcal{J}(t)$ and $\Delta\Theta(t)$. We find

$$\frac{d}{dt}\begin{pmatrix} \Delta\mathcal{J}(t) \\ \Delta\Theta(t) \end{pmatrix} = \begin{pmatrix} 0 & 4\alpha\cos(n\pi)\mathcal{J}_o(I' - \mathcal{J}_o) \\ (6 - 2\alpha\cos(n\pi)) & 0 \end{pmatrix} \times \begin{pmatrix} \Delta\mathcal{J}(t) \\ \Delta\Theta(t) \end{pmatrix}. \tag{2.4.12}$$

The solution $\binom{\Delta\mathcal{J}(t)}{\Delta\Theta(t)}$ to Eq. (2.4.12) determines the manner in which trajectories flow *in the neighborhood of the fixed points.* For $\alpha \ll 1$ (and therefore $\mathcal{J}_o \approx \frac{I'}{6}$), these equations reduce to

$$\frac{d}{dt}\begin{pmatrix} \Delta\mathcal{J}(t) \\ \Delta\Theta(t) \end{pmatrix} \approx \begin{pmatrix} 0 & \frac{20\alpha I'^2}{36}\cos(n\pi) \\ 6 & 0 \end{pmatrix}\begin{pmatrix} \Delta\mathcal{J}(t) \\ \Delta\Theta(t) \end{pmatrix}. \tag{2.4.13}$$

Let us assume that Eq. (2.4.13) has a solution of the form

$$\begin{pmatrix} \Delta\mathcal{J}(t) \\ \Delta\Theta(t) \end{pmatrix} = e^{\lambda t} \begin{pmatrix} A_{\mathcal{J}} \\ A_{\Theta} \end{pmatrix}, \tag{2.4.14}$$

where $A_{\mathcal{J}}$ and A_{Θ} are independent of time. Then we can solve the resulting eigenvalue equation

$$\lambda \begin{pmatrix} A_{\mathcal{J}} \\ A_{\Theta} \end{pmatrix} = \begin{pmatrix} 0 & \frac{20\alpha I'^2}{36}\cos(n\pi) \\ 6 & 0 \end{pmatrix} \begin{pmatrix} A_{\mathcal{J}} \\ A_{\Theta} \end{pmatrix}$$

for both λ and $\begin{pmatrix} A_{\mathcal{J}} \\ A_{\Theta} \end{pmatrix}$. The eigenvalues are given by

$$\lambda_{\pm} = \pm \left(\frac{20\alpha I'^2 \cos(n\pi)}{6} \right)^{\frac{1}{2}},$$

and the solution to Eq. (2.4.13) can be written

$$\begin{pmatrix} \Delta\mathcal{J}(t) \\ \Delta\Theta(t) \end{pmatrix} = e^{\lambda_+ t}\, A_+ \begin{pmatrix} \frac{b}{\lambda_+} \\ 1 \end{pmatrix} + e^{\lambda_- t}\, A_- \begin{pmatrix} \frac{b}{\lambda_-} \\ 1 \end{pmatrix}, \tag{2.4.15}$$

where $b = \frac{20\alpha I'^2}{36}$, and A_+ and A_- are determined by the initial conditions. For n even, λ is real and the solutions contain exponentially growing and decreasing components, while for n odd, λ is pure imaginary and the solutions are oscillatory. For n even, the fixed points are hyperbolic (trajectories approach or recede from the fixed point exponentially), while for n odd, the fixed points are elliptic (trajectories oscillate about the fixed point).

For *very small* α, the fixed points occur for $\mathcal{J}_2 = \mathcal{J}_o \approx \frac{I'}{6}$ and therefore for $J_1 \approx \frac{5I'}{6}$ and $J_2 \approx \frac{I'}{6}$. We can also find the range of energies for which these fixed points exist. Plugging $J_1 = 5J_2$ into Eq. (2.4.6), we find $J_1^2 - \frac{10J_1}{13} + \frac{25E}{39} = 0$ or $J_1 = \frac{5}{13}(1 \pm (1 - \frac{13E}{3})^{\frac{1}{2}}) = 5J_2$. Thus, the fixed points only exist for $E < \frac{3}{13}$ for very small α. For $E > \frac{3}{13}$, J_1 is no longer real.

A plot of some of the trajectories on the energy surface, $E = 0.18$, for coupling constant $\alpha = 0.1$, is given in Fig. 2.4.1. In this plot, we have transformed from polar coordinates $(\mathcal{J}_2, \Theta_2)$ to Cartesian coordinates (p, q) via the canonical transformation $p = -(2\mathcal{J}_2)^{\frac{1}{2}} \sin(\Theta_2)$ and $q = (2\mathcal{J}_2)^{\frac{1}{2}} \cos(\Theta_2)$. The elliptic and hyperbolic fixed points and the separatrix associated with them can be seen clearly. The region inside and in the immediate neighborhood outside the separatrix is called the (2,2) nonlinear resonance zone. We see that large changes in the action, $\mathcal{J}_2$, occur in this region of the phase space, indicating that a strong exchange of energy is occurring between the modes of the system.

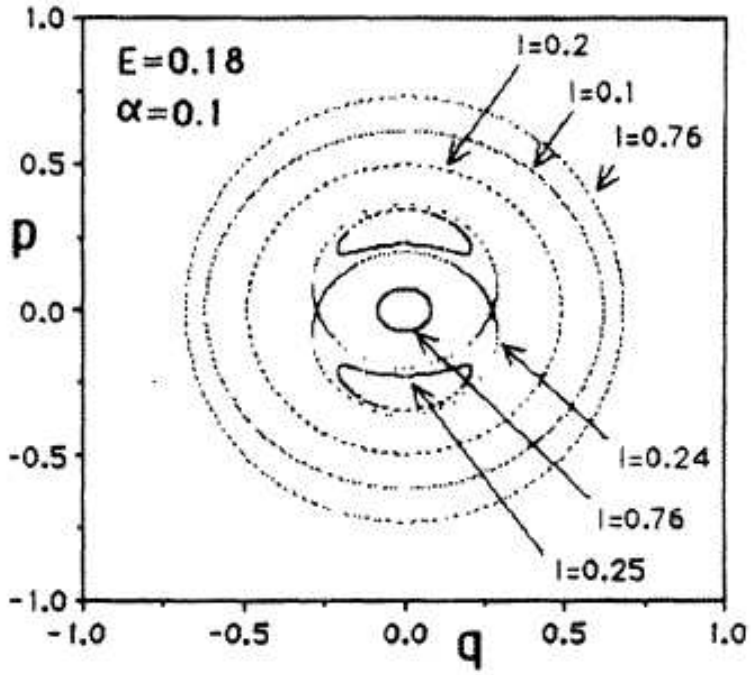

Figure 2.4.1. Phase space trajectories for the (2,2) resonance Hamiltonian in Eq. (2.4.8) ($p = -(2\mathcal{J}_2)^{\frac{1}{2}} \sin(\Theta_2)$ and $q = (2\mathcal{J}_2)^{\frac{1}{2}} \cos(\Theta_2)$). For all curves, $E = 0.18$ and $\alpha = 0.1$. The curves consist of discrete points because we have plotted points along the trajectories at discrete times.

Let us now attempt to compute these level curves using perturbation theory as discussed earlier. We go from action-angle variables $(J_1, J_2, \theta_1, \theta_2)$ to new variables $(\mathcal{I}_1, \mathcal{I}_2, \phi_1, \phi_2)$ via a canonical transformation given by the generating function

$$G(\mathcal{I}_1, \mathcal{I}_2, \phi_1, \phi_2) = \mathcal{I}_1\theta_1 + \mathcal{I}_2\theta_2 + \alpha g_{2,2}(\mathcal{I}_1, \mathcal{I}_2)\sin(2\theta_1 - 2\theta_2). \quad (2.4.16)$$

Following the procedure outlined in Sect. 2.2, we find that $g_{2,2} = \frac{-\mathcal{I}_1\mathcal{I}_2}{(2\omega_1 - 2\omega_2)}$, where $\omega_1 = 1 - 2\mathcal{I}_1 - 3\mathcal{I}_2$ and $\omega_2 = 1 - 3\mathcal{I}_1 + 2\mathcal{I}_2$. The Hamiltonian to order α^2 is $H = H_o(\mathcal{I}_1, \mathcal{I}_2) + O(\alpha^2)$ and the action variables (neglecting terms of order α^2) are

$$J_1(t) = \mathcal{I}_1 - \frac{2\alpha\mathcal{I}_1\mathcal{I}_2\cos(2\omega_1 t - 2\omega_2 t)}{(2\omega_1 - 2\omega_2)} \quad (2.4.17)$$

and

$$J_2(t) = \mathcal{I}_2 + \frac{2\alpha\mathcal{I}_1\mathcal{I}_2\cos(2\omega_1 t - 2\omega_2 t)}{(2\omega_1 - 2\omega_2)}. \quad (2.4.18)$$

In order for these equations to have meaning, the following condition must hold:

$$|2\omega_1 - 2\omega_2| = |2\mathcal{I}_1 - 10\mathcal{I}_2| \gg 2\alpha\mathcal{I}_1\mathcal{I}_2.$$

However, near a resonance, $\mathcal{I}_1 \approx 5\mathcal{I}_2$. Therefore this condition breaks down in the neighborhood of a resonance zone. Actually this is to be expected since the resonance introduces a topological change in the flow pattern in the phase space.

(2,3) Resonance

Walker and Ford also studied a (2,3) resonance with Hamiltonian

$$H = H_o(J_1, J_2) + \beta J_1 J_2^{\frac{3}{2}} \cos(2\theta_1 - 3\theta_2) = E. \tag{2.4.19}$$

This again is integrable and has two isolating integrals of the motion, the Hamiltonian, H, and

$$I = 3J_1 + 2J_2 = C_3. \tag{2.4.20}$$

We can again make a canonical transformation, $J_1 = \mathcal{J}_1 - \frac{2}{3}\mathcal{J}_2, J_2 = \mathcal{J}_2, \theta_1 = \Theta_1, \theta_2 = \Theta_2 + \frac{2}{3}\Theta_1$ (note that $I = 3\mathcal{J}_1$). The Hamiltonian then takes the form

$$\mathcal{H} = \mathcal{J}_1 - \mathcal{J}_1^2 + \frac{\mathcal{J}_2}{3} - \frac{5\mathcal{J}_1\mathcal{J}_2}{3} + \frac{23}{9}\mathcal{J}_2^2 + \frac{\beta}{3}\mathcal{J}_2^{\frac{3}{2}}(3\mathcal{J}_1 - 2\mathcal{J}_2)\cos(3\Theta_2) = E \tag{2.4.21}$$

and the coordinate $\mathcal{J}_1$ is a constant of the motion since $\mathcal{H}$ is independent of Θ_1. The equations of motion for $\mathcal{J}_2$ and Θ_2 are

of Θ_1. The equations of motion for $\mathcal{J}_2$ and Θ_2 are

$$\frac{d\mathcal{J}_2}{dt} = \beta \mathcal{J}_2^{\frac{3}{2}} (3\mathcal{J}_1 - 2\mathcal{J}_2) \sin(3\Theta_2) \tag{2.4.22}$$

and

$$\frac{d\Theta_2}{dt} = \frac{1}{3} - \frac{5\mathcal{J}_1}{3} + \frac{46\mathcal{J}_2}{9} + \beta \mathcal{J}_2^{\frac{1}{2}} \left(\frac{3}{2}\mathcal{J}_1 - \frac{5}{3}\mathcal{J}_2 \right) \cos(3\Theta_2). \tag{2.4.23}$$

It is easy to see that the fixed points occur for $\Theta_2 = \frac{n\pi}{3}$ and $\mathcal{J}_2 = \mathcal{J}_o$ where $\mathcal{J}_o$ satisfies the equation

$$\frac{1}{3} - \frac{5I}{9} + \frac{46\mathcal{J}_o}{9} + \beta \mathcal{J}_o^{\frac{1}{2}} \left(\frac{I}{2} - \frac{5}{3}\mathcal{J}_o \right) \cos(n\pi) = 0. \tag{2.4.24}$$

If we again linearize the equations of motion about these fixed points and determine the form of the flow in their neighborhood as we did below Eq. (2.4.11), we find that for even n ($n = 0, 2, 4$) the fixed points are hyperbolic while for odd n ($n = 1, 3, 5$) the fixed points are elliptic. These fixed points are clearly seen in the plot of the phase space trajectories for the (2,3) resonance system given in Fig. 2.4.2. In Fig. 2.4.2 all curves have energy $E = 0.18$ and coupling constant $\beta = 0.1$. The separatrix of the (2,3) resonance zone is clearly seen, as are the three hyperbolic and elliptic fixed points.

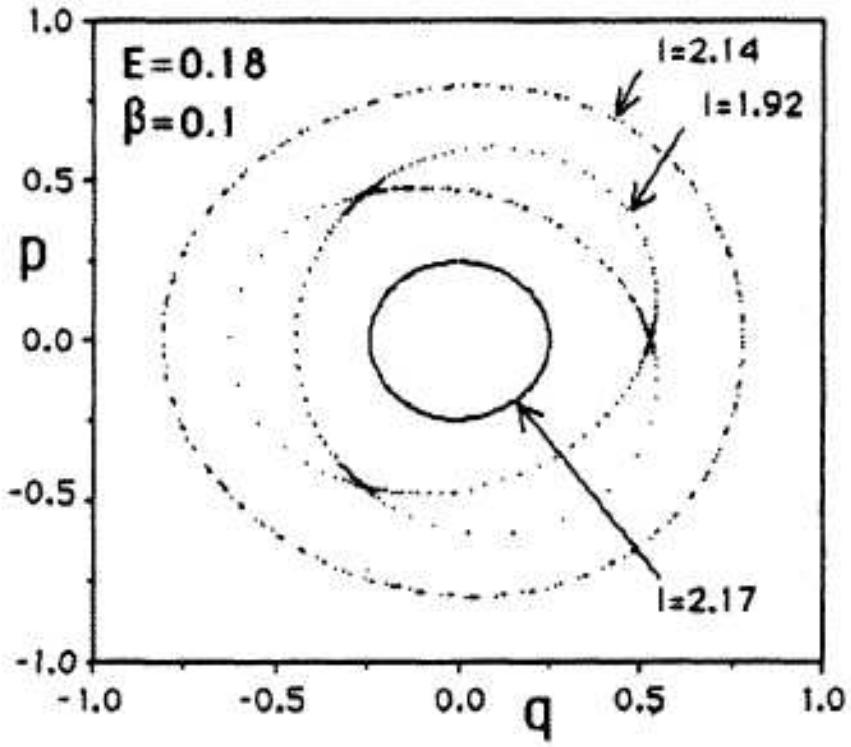

Figure 2.4.2. A plot of some phase space trajectories obtained for the (2,3) resonance Hamiltonian in Eq. (2.4.19). All curves have energy $E = 0.18$ and coupling constant $\beta = 0.1$ but have different values of the constant of motion, I. The three hyperbolic and three elliptic fixed points as well as the separatrix of the (2,3) resonance are clearly seen. The curves consist of discrete points because we plot points along the trajectories at discrete times. We have set $p = -(2\mathcal{J}_2)^{\frac{1}{2}} \sin(\Theta_2)$ and $q = (2\mathcal{J}_2)^{\frac{1}{2}} \cos(\Theta_2)$.

2.4.2 Two-Resonance Hamiltonian

$$H = H_o(J_1, J_2) + \alpha J_1 J_2 \cos(2\theta_1 - 2\theta_2) + \beta J_1 J_2^{\frac{3}{2}} \cos(2\theta_1 - 3\theta_2) = E. \tag{2.4.25}$$

Hamilton's equations for the two-resonance system can be written

$$\frac{dJ_1}{dt} = -\frac{\partial H}{\partial \theta_1} = 2\alpha J_1 J_2 \sin(2\theta_1 - 2\theta_2)$$
$$+ 2\beta J_1 J_2^{\frac{3}{2}} \sin(2\theta_1 - 3\theta_2), \tag{2.4.26}$$
$$\frac{dJ_2}{dt} = -\frac{\partial H}{\partial \theta_2} = -2\alpha J_1 J_2 \sin(2\theta_1 - 2\theta_2)$$
$$- 3\beta J_1 J_2^{\frac{3}{2}} \sin(2\theta_1 - 3\theta_2), \tag{2.4.27}$$
$$\frac{d\theta_1}{dt} = \frac{\partial H}{\partial J_1} = 1 - 2J_1 - 3J_2 + \alpha J_2 \cos(2\theta_1 - 2\theta_2)$$
$$+ \beta J_2^{\frac{3}{2}} \cos(2\theta_1 - 3\theta_2), \tag{2.4.28}$$
$$\frac{d\theta_2}{dt} = \frac{\partial H}{\partial J_2} = 1 - 3J_1 + 2J_2 + \alpha J_1 \cos(2\theta_1 - 2\theta_2)$$
$$+ \frac{3}{2}\beta J_1 J_2^{\frac{1}{2}} \cos(2\theta_1 - 3\theta_2). \tag{2.4.29}$$

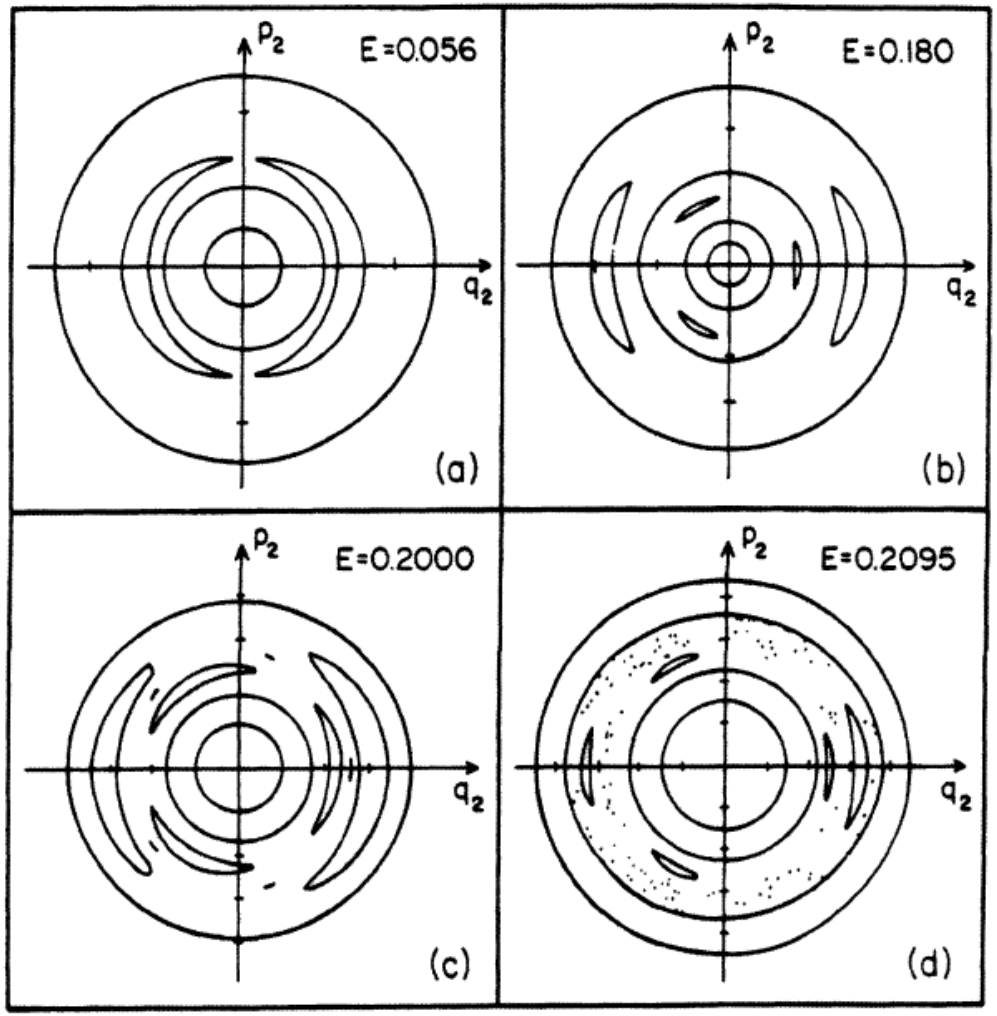

Figure 2.4.3. Poincaré surfaces of section for the double-resonance Hamiltonian in Eq. (2.4.25) with $p_2 = -(2J_2)^{\frac{1}{2}} \sin(\theta_2)$ and $q_2 = (2J_2)^{\frac{1}{2}} \cos(\theta_2)$ and coupling constants $\alpha = \beta = 0.02$. (a) At energy $E = 0.056$, only the (2,2) resonance exists. (b) At energy $E = 0.180$, the (2,3) resonance has emerged from the origin but is well-separated from the (2,2) resonance. (c) At energy $E = 0.2000$, the two primary resonances have grown in size but remain separated. The chain of five islands is a higher-order resonance. (d) At energy $E = 0.2095$, resonance overlap has occurred and chaos can be seen in the overlap region. [Walker and Ford 1969]

Walker and Ford construct a Poincaré surface of section by solving the equations of motion (2.4.26)–(2.4.29) numerically and plotting (J_2, θ_2) each time $\theta_1 = \frac{3\pi}{2}$. (If $p_i = -(2J_i)^{\frac{1}{2}} \sin(\theta_i)$ and $q_i = (2J_i)^{\frac{1}{2}} \cos(\theta_i)$, the surface of section is similar to that of Henon and Heiles, who plot a point (p_2, q_2) each time $q_1 = 0$ and $p_1 > 0$.) A sketch of the Poincaré surface of section for several energies is shown in Fig. 2.4.3. In all cases shown in this figure, the coupling constants are $\alpha = \beta = 0.02$, a value much smaller than those used in Figs. 2.4.1 and 2.4.2. The (2,2) resonance is present for all energies $E \leq \frac{3}{13}$. However, the (2,3) resonance first emerges from the origin for energy $E \approx 0.16$. For energies $E = 0.056$ (Fig. 2.4.3.a), only the (2,2) resonance exists. For $E = 0.180$ (Fig. 2.4.3.b), both resonances are present but well-separated in the phase space. As the energy is raised, the resonances occupy larger regions of the phase space. Finally, for $E = 0.2095$ (Fig. 2.4.3.d), the resonances have overlapped and a chaotic trajectory is found.